RSC Advances

ROYAL SOCIETY OF CHEMISTRY

www.rsc.org/advances

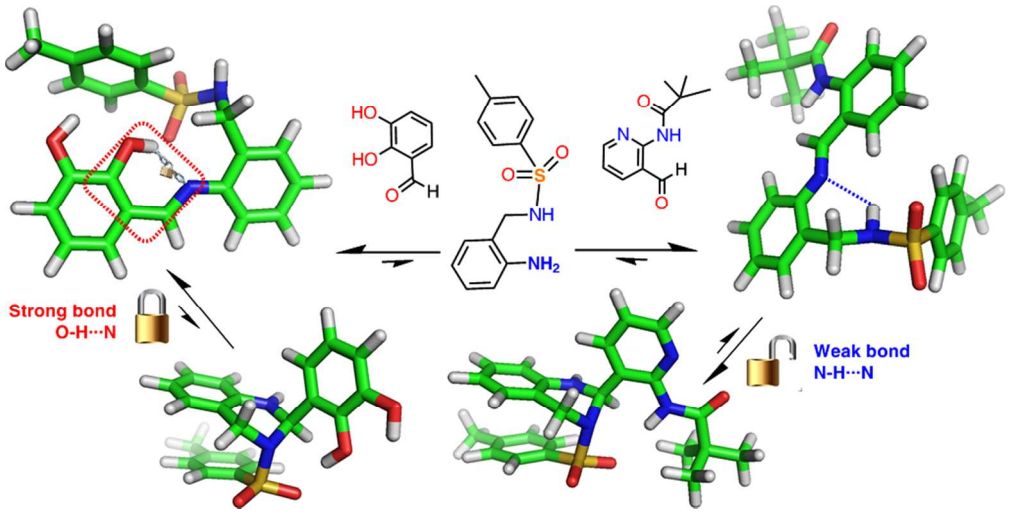

Adequate substituents can favour/hinder, the tautomerisation of Schiff bases into tetrahydroquinazolines, by means of strong/weak H bonds
269x135mm (96 x 96 DPI)

Cite this: DOI: 10.1039/c0xx00000x

www.rsc.org/xxxxxx

ARTICLE TYPE

Controlling ring-chain tautomerism through steric hindrance

Ana M. García-Deibe,[a] Cristina Portela-García,[a] Matilde Fondo[a] and Jesús Sanmartín-Matalobos[a,*]

Received (in XXX, XXX) Xth XXXXXXXXX 20XX, Accepted Xth XXXXXXXXX 20XX
DOI: 10.1039/b000000x

We have explored the use of steric hindrance for favouring/hindering the tautomerisation of Schiff bases (SB) into tetrahydroquinazolines (TQ) in two systems that derive from the condensation of 2-tosylaminobenzylamine with two different aldehydes: 2,3-dihydroxybenzaldehyde ($H_2L^1{}_{SB}/H_2L^1{}_{TQ}$) and *N*-(3-formylpyridin-2-yl)pivalamide ($H_2L^2{}_{SB}/H_2L^2{}_{TQ}$). The four possible ring-chain tautomers were unequivocally characterised by a combination of ^{1}H NMR spectroscopy, infrared spectroscopy, mass pectrometry and elemental analysis. Furthermore, two of the tautomers, $H_2L^1{}_{SB}$ and $H_2L^2{}_{TQ}$, have been characterised by X-ray crystallography. Crystal data of *E*-$H_2L^1{}_{SB}$ have revealed the existence of a prototropic ketoenamine–enolimine equilibrium at room temperature that is the cause of the thermochromism of $H_2L^1{}_{SB}$. A firm intramolecular interaction $O_{hydroxyl}$-H···N_{imine} hinders the conversion of the chain tautomer $H_2L^1{}_{SB}$ into the ring tautomer $H_2L^1{}_{TQ}$. Crystals of $H_2L^2{}_{TQ}$ and $H_2L^2{}_{TQ}$·$HCCl_3$ consist of racemic mixtures of their enantiomers, C(*R*),N(*R*)-$H_2L^2{}_{TQ}$ and C(*S*),N(*S*)-$H_2L^2{}_{TQ}$. A terminal pivalamide group prevents the existence of the intramolecular interaction $N_{pivalamide}$-H···N_{imine} in the chain tautomer $H_2L^2{}_{SB}$, favouring its conversion into the ring tautomer $H_2L^2{}_{TQ}$.

Introduction

Tautomerism plays a very important role in organic chemistry, medicinal chemistry, pharmacology, biochemistry, molecular biology and in life itself.[1-7] Understanding and controlling tautomerisations is very important for synthesis and reactivity of many organic and metal-organic compounds.[8,9] Ring-chain tautomerism is a particular kind of structural isomerism, where a hydrogen atom migration is followed by a change from an open chain to a ring in molecular structure.

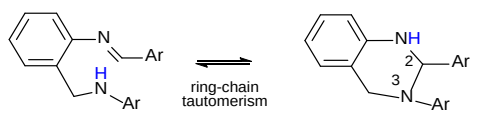

Schiff base (SB) Tetrahydroquinazoline (TQ)

Scheme. 1. Ring-chain tautomerism of an Schiff base/tetrahydroquinazoline system by reversible intramolecular nucleophilic addition of the $N^{-\delta}{}_{amine}$ atom to the electrophilic sp^2-hybridised $C^{+\delta}{}_{imine}$ atom associated with the migration of an H atom (in blue colour).

The ring-chain tautomerism of 2,3-diaryl-1,2,3,4-tetrahydroquinazolines (scheme 1) was reported first thirteen years ago.[10] Fülöp and co-workers found that the ring-chain ratio depends on the electronic character (σ^+) of the substituent on the 2-aryl ring (Hammett-type eq.).[10] Sinkkonen,[11] explained the preference for the chain tautomeric form in some Schiff base/tetrahydroquinazoline systems by intramolecular H bonds between amine and imine functional groups.

Recently, we have found that the ring-chain ratio for 2-aryl-3-tosyl-1,2,3,4-tetrahydroquinazolines depends on the reaction time.[12,13]. Thus, reaction times of about 1 h gave the open-chain tautomer as the main product, however, as time goes on, the ring-chain ratio is increasing, and after several hours the ring tautomer is clearly the most abundant product in the brute. DFT calculations evidenced that the intramolecular ring-closing reaction is energetically favoured in the 2,3-diaryl-1,2,3,4-tetrahydroquinazoline studied by us.[12]

Now, we have focused our attention on controlling tautomerisation of imines into tetrahydroquinazolines through steric hindrance. With this purpose, we have studied by using X-ray crystallography and nuclear overhauser enhancement spectroscopy (NOESY) in combination with molecular mechanics modelling, the structural features of each one of the tautomers obtained from separate reactions of 2-tosylaminobenzylamine[14] with 2,3-dihydroxybenzaldehyde and *N*-(3-formylpyridin-2-yl)pivalamide (scheme 2). We have selected the systems $H_2L^1{}_{SB}/H_2L^1{}_{TQ}$ and $H_2L^2{}_{SB}/H_2L^2{}_{TQ}$ for two reasons: i) the steric hindrance that the pivalamide functional group can exert to avoid the existence of the interaction $N_{pivalamide}$-H···N_{imine} in $H_2L^2{}_{SB}$, and ii) the enhanced strength of the intramolecular bond $O_{hydroxyl}$-H···N_{imine}, which can prevail over $N_{sulfonamide}$-H···N_{imine} in $H_2L^1{}_{SB}$.[15,16] Since OH···N bonds are usually stronger than NH···N ones,[17-20] the stabilisation of the chain tautomer $H_2L^1{}_{SB}$ can be due to intramolecular H bonds between -OH and -HC=N- groups rather than between –$NHSO_2$- and -HC=N- groups.

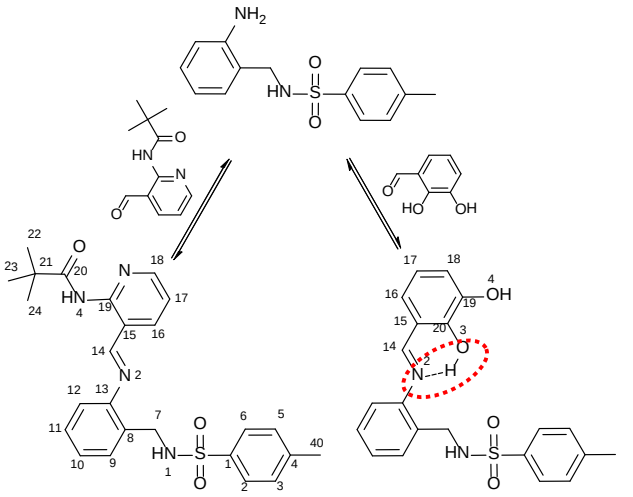

Scheme. 2. Schematic representation of the Schiff bases $H_2L^1_{SB}$ (right) and $H_2L^2_{SB}$ (left), which were obtained from separate reactions of 2-tosylaminobenzylamine with 2,3-dihydroxybenzaldehyde and *N*-(3-formylpyridin-2-yl)pivalamide, respectively. The strong intramolecular hydrogen bond O-H···N in $H_2L^1_{SB}$ is highlighted. The numbering scheme for NMR is shown.

Discussion

Studies on the $H_2L^1_{SB}/H_2L^1_{TQ}$ system

Condensation reaction of 2,3-dihydroxybenzaldehyde and 2-tosylaminomethylaniline[14] occurs efficiently in methanol solution, leading to the Schiff base $H_2L^1_{SB}$. The 2-D NOESY spectrum of $H_2L^1_{SB}$ (Fig. 1, bottom) shows the cross peaks due to the coupling of the imine proton (H-14) with aromatic protons H-12 and H-16, as well as those due to the coupling of the methylene H atoms (H-7) with tosyl and aniline residues (H-2,6 and H-9, respectively). In view of the considerable rigidity of $H_2L^1_{SB}$, these few couplings allow elucidating the conformation adopted by $H_2L^1_{SB}$ in solution. We have used molecular mechanics modelling to obtain the lowest energy conformation of $H_2L^1_{SB}$ that is coherent with the experimentally observed couplings by ^{1}H NMR spectroscopy in solution (Fig. 1, top). This conformation shows an *E* configuration with a strong intramolecular hydrogen bond between -OH and -HC=N- groups (O3···N2 length about 2.60 Å). One might note that this short N···O length can be related to an estimated bond energy[20] around 10 kcal mol^{-1}.The enhanced strength of this bond appears to be the cause for the stabilisation of the enolimine form, preventing the tautomerisation of $H_2L^1_{SB}$ into $H_2L^1_{TQ}$, even under reflux for 4 h.

With the aim of verifying the existence of the O3···N2 interaction in solid state, we have cooled a powdery sample of $H_2L^1_{SB}$ in liquid nitrogen. As a result, we have observed a fast and reversible change that consists on an immediate fading of the colour of the powder, from deep orange at room temperature to yellowish orange at liquid nitrogen temperature (scheme 3, top). This thermochromic behaviour,[1,2,15] which is controlled by the enhanced basicity of the imine nitrogen due to the absence of conjugation with the phenyl ring, is an evident sign of the dynamically disordered bonds N–H···O ⇄ O–H···N (scheme 3, bottom).

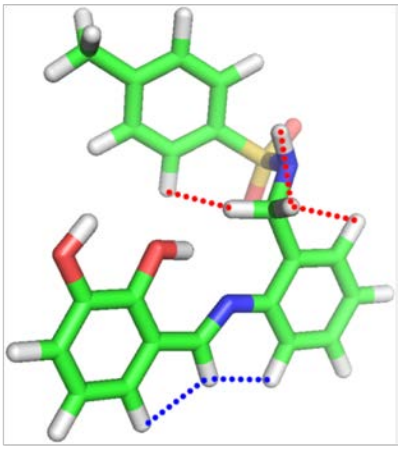

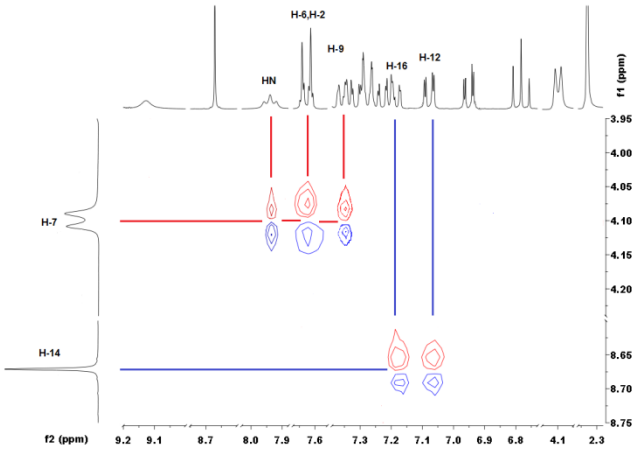

Fig. 1. *Bottom:* Partial view of the NOESY spectrum of $H_2L^1_{SB}$ highlighting the most relevant cross peaks used to the structural diagnosis. *Top*: The most stable conformation of $H_2L^1_{SB}$ that is coherent with the experimentally observed couplings. Lines of same colours highlight the H-H couplings in both NOESY spectrum and sticks sketch.

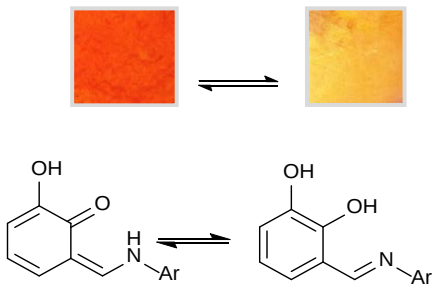

Scheme 3. *Top*: Photographs of a powdery sample of $H_2L^1_{SB}$ at room temperature (left), and after immersion in liquid nitrogen (right). *Bottom*: Prototropic ketoenamine–enolimine equilibrium of $H_2L^1_{SB}$.

The fading of the powdery sample with lowering of temperature is a clear sign of a change of the enolimine - ketoenamine–ratio.[2,15,21,22] In fact, as the crystal

structure obtained indicates (see below), both species are coexisting at room temperature. Despite this, we have only observed the typical bands of the enolimine form in the infrared spectrum of $H_2L^1_{SB}$ (ESI).[16]

Fig. 2 shows the molecular structure of $H_2L^1_{SB}$ provided by single crystal X-ray diffraction techniques at room temperature. The labelling scheme used in this figure has been also employed to identify the corresponding NMR signals. As expected, $H_2L^1_{SB}$ displays a typical *E* configuration in solid state. This is favoured by a strong intramolecular H bond between the -OH group located at 2-position of the aldehyde residue and the -HC=N- group.

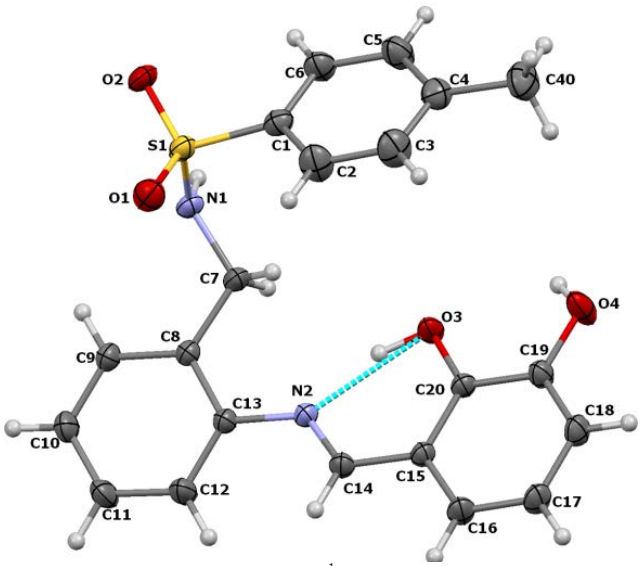

Fig. 2. Molecular structure of *E*-$H_2L^1_{SB}$ with its labelling scheme. The strong intramolecular O3···N2 interaction, with the most occupied position for H3 (67%) is shown.

The most significant bond distances and angles (ESI) corresponding to the 2-tosylaminomethylaniline residue show that geometric parameters fall within the usual ranges for related compounds.[12,13] With regard to the aldehyde residue, the short length of the O3-H3···N2 interaction (2.56 Å) provides evidence of its intensity, allowing its qualification as strong intramolecular resonance-assisted H-bond (RAHB).[15-18] A hydrogen atom, with occupation sites about 67% and 33%, has been found near to O3 (H3p) and N2 (H3a), respectively. This shows the existence of the dynamically disordered hydrogen bonds O3−H3P···N2 and N2−H3A···O3. Besides, C20-O3 is shorter than 1.37 Å, which is the expected value for pure enolimines.[2,21,22] At the same time, C13-N2 is shorter than 1.47 Å, what is indicative of some double bond character. Since diffraction data are an average of the geometric parameters of those molecules present in the crystal, we have demonstrated that at room temperature exists a prototropic ketoenamine–enolimine equilibrium (scheme 3) that favours the enolimine form (ketoenamine–enolimine ratio about 0.5) at room temperature.

With the aim of studying the changes with time in ring-chain ratio at room temperature, a spectroscopic monitoring of a dimethylsulfoxide solution of $H_2L^1_{SB}$ has been performed (ESI). After three days, a ring-chain ratio about 0.1 has been detected, showing a very slow tautomerisation of $H_2L^1_{SB}$ into the ring tautomer $H_2L^1_{TQ}$. This tautomerisation is concomitant with gradual decomposition of $H_2L^1_{SB}$ by imine hydrolysis. The explanation for the interconversion of tautomers in solution seems to lie in low tautomerisation barriers.

The NOESY spectrum of $H_2L^1_{TQ}$ (Fig. 3, bottom) reveals the cross peaks due to the coupling of the equatorial methylene proton (H-7_{eq}) with H-9 of the aniline residue (red line). Besides, the axial methylene proton (H-7_{ax}) is coupled with H-16 of the aldehyde residue (blue line). Fig. 3, at the top, shows the lowest energy conformation of $H_2L^1_{TQ}$ that is coherent with the experimentally observed couplings by ^{1}H NMR spectroscopy in solution. Since the O3-H··N1 distance in the molecular model is about 2.95 Å not very significant intramolecular H bond seems to stabilise the ring tautomer.

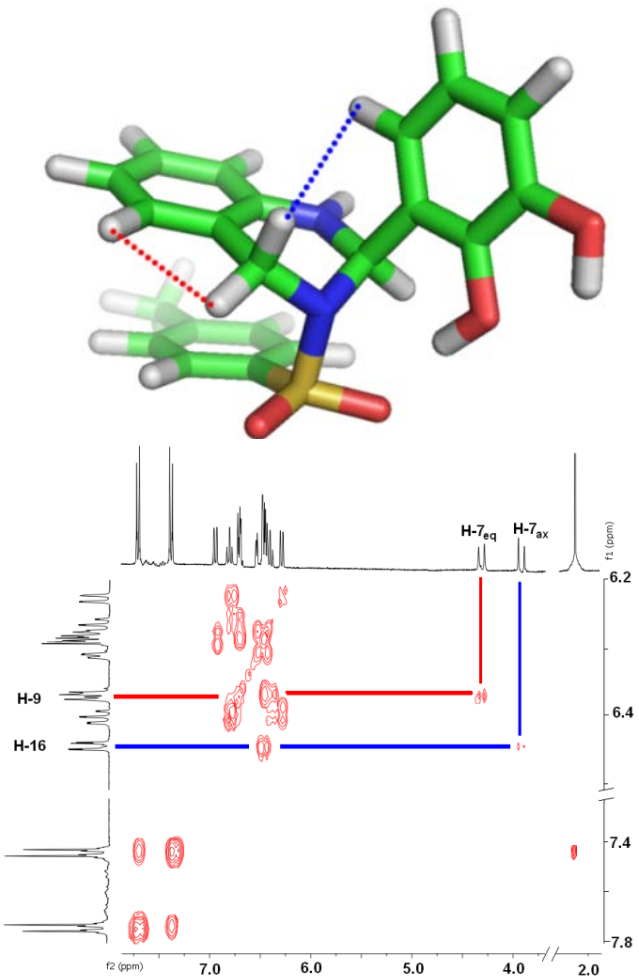

Fig. 3. *Bottom:* Partial view of the NOESY spectrum of $H_2L^1_{TQ}$ highlighting the most relevant cross peaks used to the structural diagnosis. *Top*: The most stable conformation of $H_2L^1_{TQ}$ (obtained from molecular mechanics modelling) that is coherent with the experimentally observed couplings. Lines of same colours highlight the H-H couplings in both NOESY spectrum and sticks sketch.

Studies on the $H_2L^2_{SB}/H_2L^2_{TQ}$ system

Condensation reaction of *N*-(3-formylpyridin-2-yl)pivalamide and 2-tosylaminomethylaniline[14] occurs efficiently in chloroform

solution, but contrary to the observed for the $H_2L^1{}_{SB}/H_2L^1{}_{TQ}$ system, the crystallised reaction product is the ring tautomer, $H_2L^2{}_{TQ}$. As expected, $H_2L^2{}_{TQ}$ results from the intramolecular nucleophilic addition of the $N^{-\delta}{}_{amine}$ atom to the electrophilic $C^{+\delta}{}_{imine}$ atom of $H_2L^2{}_{SB}$, and therefore some residual amount of $H_2L^2{}_{SB}$ can be detected by NMR spectroscopy in the brute.

The NOESY spectrum of $H_2L^2{}_{TQ}$ (Fig. 4, bottom) shows the cross peaks due to the coupling of the pivalamide proton (HN-4) with methanetriyl proton (H-14) and H_{methyl}, (H-22, H-23 and H-24) as well as those due to the coupling of the equatorial methylene proton ($H\text{-}7_{eq}$) with H-2,6 of the tosyl group (blue line) and H-9 of the aniline residue (red line). Besides, the axial methylene proton ($H\text{-}7_{ax}$) is coupled with H-16 of the pyridine ring (orange line). We have used molecular mechanics modelling to obtain the lowest energy conformation of $H_2L^2{}_{TQ}$ that is coherent with the experimentally observed couplings by ^{1}H NMR spectroscopy in solution (Fig. 4, top). Although $H_2L^2{}_{TQ}$ is a chiral compound, and therefore both *S* and *R* enantiomers can coexist, we have only represented the latter one in Fig. 4 (top), for clarity. Since the N4-H··N1 distance in the molecular model is about 2.86 Å, not very significant intramolecular H bond seems to stabilise the ring tautomer.

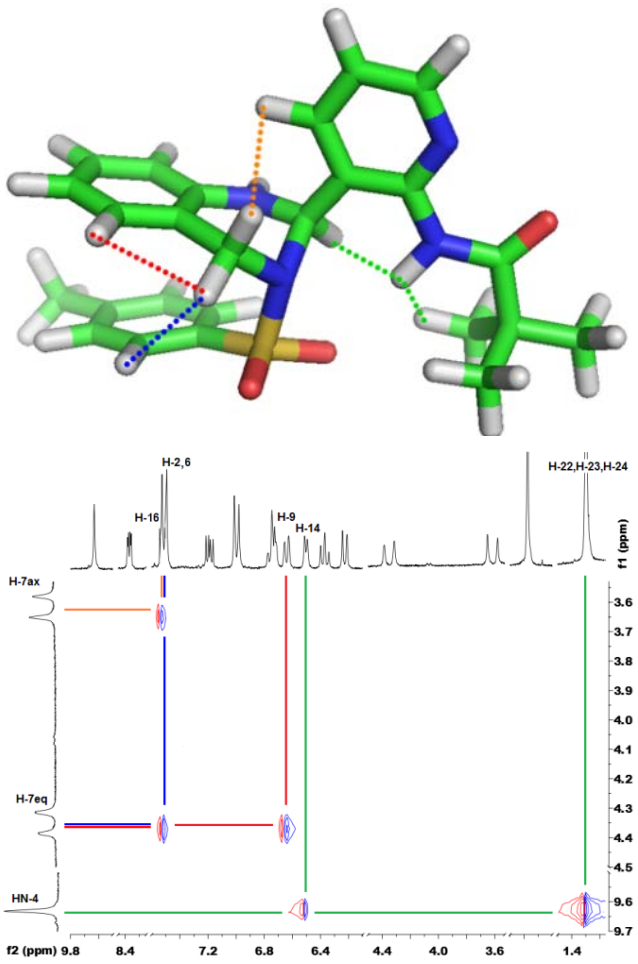

Fig. 4. *Bottom:* Partial view of the NOESY spectrum of $H_2L^2{}_{TQ}$ highlighting the most relevant cross peaks used to the structural diagnosis. *Top*: The most stable conformation of $H_2L^2{}_{TQ}$ that is coherent with the experimentally observed couplings. Lines of same colours highlight the H-H couplings in both NOESY spectrum and sticks sketch.

Apart from C14, $H_2L^2{}_{TQ}$ shows another centre that can be considered as chiral, the sulfonamide N-atom (N1), although one might note that its inversion could be possible. Therefore, we have used molecular mechanics modelling to obtain the resulting conformation of $H_2L^2{}_{TQ}$. The structural changes involved in the hypothetical inversion of N1 would imply a change from an equatorial to an axial position of the methanetriyl proton (H-14). As the coupling between axial methylene proton ($H\text{-}7_{ax}$) and methanetriyl proton (H-14) was not observed, we have dismissed the presence in solution of the enantiomeric pair C(*R*),N(*S*) and C(*S*),N(*R*), which would be resulting conformations with inversion of N1 (ESI).

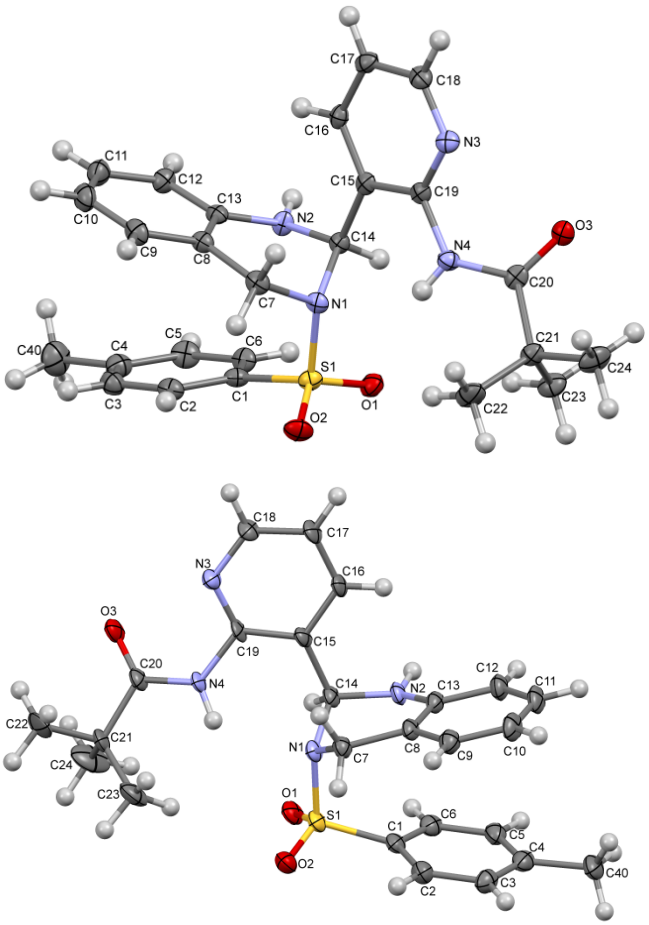

Fig. 5. Molecular structures of the enantiomers C(*R*),N(*R*) (top) and C(*S*),N(*S*) (bottom) of $H_2L^2{}_{TQ}$. These have been found for *rac*-$H_2L^2{}_{TQ}$·$HCCl_3$ (solvated chloroform was omitted for clarity) and *rac*-$H_2L^2{}_{TQ}$, respectively.

Single crystal X-ray diffraction techniques have confirmed that the uncoloured crystals collected from a methanol solution of $H_2L^2{}_{TQ}$, consist of a racemic mixture of its enantiomers, C(*R*),N(*R*)-$H_2L^2{}_{TQ}$ and C(*S*),N(*S*)-$H_2L^2{}_{TQ}$ (Fig. 5). As the crystal belongs to the centrosymmetric space group *P*-1, the compound crystallises as a racemate. An attempt of crystallising the chain tautomer in chloroform led to crystals of *rac*-$H_2L^2{}_{TQ}$·$HCCl_3$ (Fig. 5). The presence of a solvated chloroform molecule makes the main difference in both asymmetric unit and crystal packing.

Bond distances and angles, which are shown in ESI, fall within the usual ranges for other tetrahydroquinazoline compounds.[12,13,23] Since the N4-H···N1 distance is about 2.89 Å and NHN angle is less than 130º, the intramolecular H bond is not very significant. One might note that the conformation of C(*R*),N(*R*)-$H_2L^2_{TQ}$ that we have obtained from X-ray diffraction data (Fig. 5, top) appears to be not very different from that displayed in solution (Fig. 4, top), as the distances between the corresponding H atoms seem to be suitable for the couplings observed in the NOESY spectrum.

The half-chair conformation, which is adopted by the tetrahydroquinazoline ring in chiral $H_2L^2_{TQ}$ (ESI), contrasts with the envelope conformation found for the achiral 3-tosyl-1,2,3,4-tetrahydroquinazoline,[24] explaining the diasterotopic nature of the methylene protons in $H_2L^2_{TQ}$ (H-7_{eq} and H-7_{ax}). Regarding to other aspects related to conformation, $H_2L^2_{TQ}$ displays the preferred conformation of sulfonamides, *i.e.*, with the lone pair of the N atom bisecting the O=S=O angle and practically perpendicular to the tosyl ring.[25]

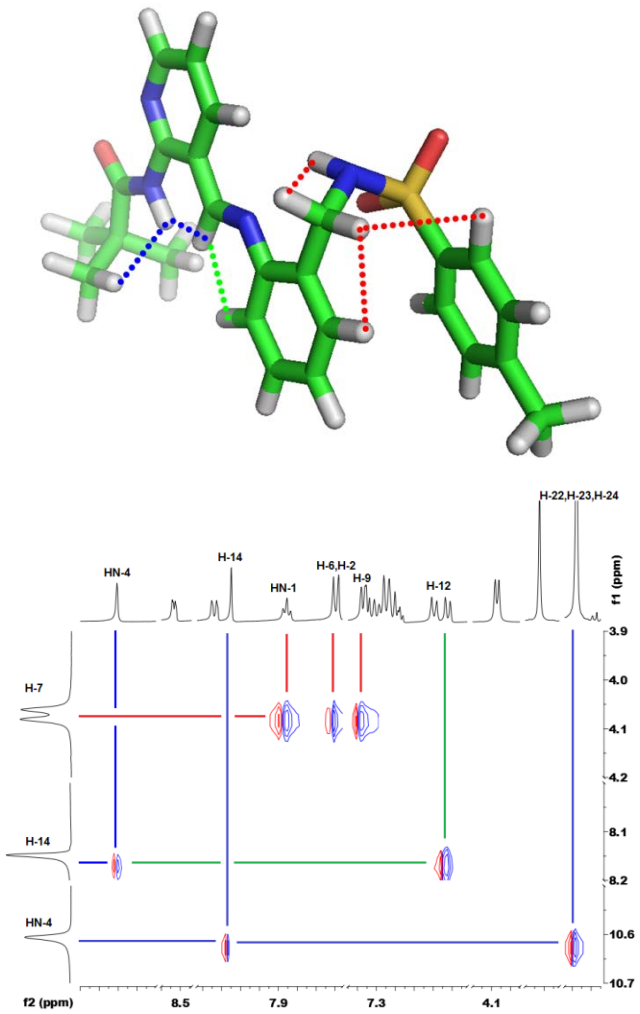

Fig. 6. *Bottom:* Partial view of the NOESY spectrum of $H_2L^2_{SB}$ highlighting the most relevant cross peaks used to the structural diagnosis. *Top*: The most stable conformation of $H_2L^2_{SB}$ that is coherent with the experimentally observed couplings. Lines of same colours highlight the H-H couplings in both NOESY spectrum and sticks sketch.

With the aim of studying the changes with time in ring-chain ratio at room temperature, a spectroscopic monitoring of a dimethylsulfoxide solution of $H_2L^2_{TQ}$ has been performed (ESI). After three days, a ring-chain ratio about 0.9 has been detected, showing a very slow tautomerisation of $H_2L^2_{TQ}$ into the chain tautomer $H_2L^2_{SB}$. This tautomerisation is followed by a gradual decomposition of $H_2L^2_{SB}$ by imine hydrolysis. These processes result in a reaction mixture that reverts to $H_2L^2_{TQ}$ after refluxing and recrystallisation. The explanation for the interconversion of tautomers in solution seems to lie in low tautomerisation barriers.

With regard to the chain tautomer $H_2L^2_{SB}$, its NOESY spectrum showed the cross peaks due to the coupling of imine proton (H-14) with both pivalamide and aniline protons (HN-4 and H-12, respectively), as well as those due to the coupling of the methylene H atoms (H-7) with tosyl and aniline residues (H-2,6 and H-9, respectively). Fig. 6, at the top, shows the lowest energy conformation of $H_2L^2_{SB}$ that is coherent with the experimentally observed couplings by ^{1}H NMR spectroscopy in solution. One might note that the steric hindrance due to the pivalamide group on the 2-position of the aldehyde residue of $H_2L^2_{SB}$ leads this tautomer to a conformation that prevents the N4-H···N2 intramolecular interaction. Since the N1-H···N2 distance is about 2.93 Å not very significant intramolecular H bond seems to stabilise the chain tautomer.

It should be noted that all preceding NMR results have been obtained in DMSO-d_6, so they should not be generalised to other solvents.

Conclusions

We have demonstrated that an adequate substituent in 2-position of the 2-aril ring can favour/hinder the tautomerisation of Schiff bases into tetrahydroquinazolines, even in solution. The obtaining of the chain tautomer is favoured by the use of a salicylaldehyde derivative, which hinders the tautomerisation of the imine into the tetrahydroquinazoline through a strong intramolecular hydrogen bonding between -OH and -HC=N- groups rather than between -$NHSO_2$- and -HC=N- groups. In contrast, the obtaining of the ring tautomer is favoured by the use of an aromatic aldehyde with a large substituent in 2'-position of the aryl ring. The steric hindrance due to the pivalamide on the 2-position of the aldehyde residue of $H_2L^2_{SB}$ leads this tautomer to a conformation that prevents the intramolecular interaction $N_{pivalamide}$-H···N_{imine}, favouring the tautomerisation of the Schiff base into the tetrahydroquinazoline.

Experimental

All the compounds were unequivocally characterised by a combination of ^{1}H NMR spectroscopy, infrared spectroscopy, mass spectrometry and elemental analysis. Furthermore, both *E*-$H_2L^1_{SB}$ and *rac*-$H_2L^2_{TQ}$ could be also crystallographically characterised.

$H_2L^1_{SB}$/$H_2L^1_{TQ}$. 2,3-dihydroxybenzaldehyde (0,15 g, 0,73 mmol) was added to an absolute ethanol solution (40 mL) of 2-tosylaminomethylaniline (0.20 g, 0.73 mmol). The resulting solution was refluxed for 4 h (or stirred at room temperature for

five days). After cooling, it was filtrated upon celite, and the resulting solution was concentrated to obtain a deep orange solid. Crystals of $H_2L^1{}_{SB}$ has been obtained by recrystallisation in methanol.

$H_2L^1{}_{SB}$. Yield: 0.27 g (92%). ^{1}H NMR (500 MHz, DMSO-d_6, δ in ppm): 12.56 (s, 1H, HO3), 9.28 (s, 1H, HO4), 8.70 (s, 1H, H-14), 8.06 (t, 1H, HN1), 7.64 (d, 2H, H-2 + H-6), 7.36 (d, 1H, H-9); 7.32 (t, 1H, H-11), 7.27 (d, 2H, H-3 + H-5); 7.23 (t, 1H, H-10), 7.17 (d, 1H, H-12), 7,08 (d, 1H, H-16), 6.96 (d, 1H, H-18), 6.79 (t, 1H, H-17), 4.10 (d, Hz, 2H, H-7), 2.34 (s, 3H, H-40). IR (KBr, ν/cm^{-1}): ν(OH) 3414, ν(NH) 3293, ν(C=N$_{imi}$) 1619, ν_{as}(SO$_2$) 1329, ν_s(SO$_2$) 1158. MS (ESI$^+$, MeOH/HCOOH) *m/z*: 419,2 (100%) $[H_2L^1+Na]^+$. Elemental analysis: C 63.8; H 5.3; N 7.0; S 8.1%; calc. for $C_{21}H_{20}N_2O_4S$: C 63.6; H 5.1; N 7.1; S 8.1%.

$H_2L^1{}_{TQ}$. ^{1}H NMR (500 MHz, DMSO-d_6, δ in ppm): 7.70 (dd, 2H, H-6 + H-2), 7.38 (dd, 2H, H-3 + H-5), 6.95 (d, 1H, H-16), 6.79 (t, 1H, H-11), 6.71 (d, 1H, H-9), 6.70 (d, 1H, H-18), 6.53 (d, 1H, H-14), 6.46 (t, 1H, H-17,), 6.43 (d, 1H, H*N*-1), 6.40 (t, 1H, H-10), 6.28 (d, 1H, H-12), 4.31 (d, 1H, H-7$_{eq}$), 3.91 (d, 1H, H-7$_{ax}$), 2.38 (s, 3H, H-40).

$H_2L^2{}_{SB}$/$H_2L^2{}_{TQ}$. *N*-(3-formylpyridin-2-yl)pivalamide (0.30 g, 1.46 mmol) was added to a chloroform solution (60 mL) of 2-tosylaminomethylaniline (0.40 g, 1.46 mmol). The resulting solution was refluxed for 4 h. After cooling, it was filtrated upon celite, and the resulting solution was concentrated to obtain a yellowish oily product. The reaction mixture was stirred with diethyl ether during 4 hours. Then it was filtrated and washed with diethyl ether obtaining a white solid. Crystals of $H_2L^2{}_{TQ}$ has been obtained by recrystallisation in methanol and also in chloroform.

$H_2L^2{}_{TQ}$. Yield: 315 mg (93 %).^{1}H NMR (500 MHz, DMSO-d_6): δ = 9.63 (s, 1H, HN-4), 8.37 (d, 1H, H-18), 7.52 (d, 1H, H-16), 7.51 (d, 2H, H-6 + H-2), 7.19 (t, 1H, H-17), 6.99 (d, 2H, H-3 + H-5), 6.75 (t, 1H, H-11), 6.74 (d, 1H, HN-2), 6.64 (d, 1H, H-9), 6.50 (d, 1H, H-14), 6.37 (t, 1H, H-10), 6.23 (d, 1H, H-12), 4.35 (d, 1H, H-7$_{eq}$), 3.61 (d, 1H, H-7$_{ax}$), 2.18 (s, 3H, H-40), 1.30 (s, 9H, H-22, H-23, H-24). IR (KBr, ν/cm^{-1}): ν(N$_{TQ}$-H) 3372, ν(N$_{pivalamide}$-H) 3297, ν(C=O) 1688, ν_{as}(SO$_2$) 1337, ν_s(SO$_2$) 1164. MS (FAB$^+$, MNBA) *m/z*: 465,2 (100%) $[H_2L^2+H]^+$. Elemental analysis: C 64.6; H 6.1; N 12.0; S 6.6; calc. for $C_{25}H_{28}N_4O_3S$: C 64.6; H 6.1; N 12.1; S 6.9 %.

$H_2L^2{}_{SB}$. ^{1}H NMR (500 MHz, DMSO-d_6, δ in ppm): 10.61 (s, 1H, HN-4), 8.53 (d, 1H, H-18), 8.24 (d, 1H, H-16), 8.15 (s, 1H, H-14), 7.86 (t, 1H, HN-1), 7.59 (d, 2H, H-2 + H-6), 7.40 (d, 1H, H-9), 7.38 (t, 1H, H-17), 7.37 (t, 1H, H-11), 7.24 (d, 2H, H-3 + H-5), 7.23 (t, 1H, H-10), 6.95 (d, 1H, H-12), 4.07 (d, 2H, H-7), 2.33 (s, 3H, H-40), 1.18 (s, 9H, H-22 + H-23 + H-24).

X-ray diffraction techniques. Orange prismatic crystals of $H_2L^1{}_{SB}$ were obtained after room temperature evaporation from a methanol solution. Colourless crystals of *rac*-$H_2L^2{}_{TQ}$ and *rac*-$H_2L^2{}_{TQ}$·$HCCl_3$, were isolated from attempts of recrystallisation of $H_2L^2{}_{TQ}$ in methanol, and $H_2L^2{}_{SB}$ in chloroform, respectively. Crystal and diffraction data are collected in Table S1 (ESI). Crystals of $H_2L^1{}_{SB}$ were measured at room temperature with Cu*K*α radiation, while data for the other two ones were collected at 100(2) K with Mo*K*α radiation. Data were processed and corrected for Lorentz, polarisation and absorption effects. The structures were solved by standard direct methods,[26] and then refined by full matrix least squares on F^2.[27] All non-hydrogen atoms were anisotropically refined. Hydrogen atoms were included in the structure factor calculation in geometrically idealised positions, with thermal parameters depending of the parent atom, by using a riding model. Those hydrogen atoms implied in the H bonding scheme were found in Fourier maps, and refined with thermal parameters depending of the parent atom.

CCDC 1402381, 1402382 and 1402383 contain the supplementary crystallographic data for this paper.

Notes and references

[a] *Dpto. Química Inorgánica. Fac. Química. Univ. Santiago de Compostela. Campus Vida. Santiago de Compostela. 15782. Spain. Tel: 34 881814396; E-mail: jesus.sanmartin@usc.es.*

† Electronic Supplementary Information (ESI) available: [crystal diffraction data, selected geometric parameters, conformations, IR spectra and ^{1}H NMR monitoring]. See DOI: 10.1039/b000000x/

1 E. D. Raczyska, W. Kosinska, B. Osmiałowski and R. Gawinecki, *Chem. Rev*. 2005, **105**, 3561

2 E. Hadjoudis and I. M. Mavridis, *Chem. Soc. Rev*. 2004, **33**, 579.

3 D. A. Iglesias, D. L. Ruiz and P. E. Allegretti, *J. Appl. Sol. Chem. Model*., 2012, **1**, 113.

4 N. M. Abdel Gawad, H. H. Georgey, R. M. Youssef and N. A. El-Sayed, *Eur. J. Med. Che*m., 2010, **45**, 6058.

5 C. Jiang, L. Yang, W.-T. Wu, Q.-L. Guo and Q.-D. You, *Bioorg. Med. Chem*. 2011, **19**, 5612.

6 K, Okumura, T. Oine, Y. Yamada , G. Hayashi and M. Nakama, *J. Med. Chem*. 1968, **11**, 348.

7 B. V. Shetty, L. A. Campanella, T. L. Thomas, M. Fedorchuk, T. A. Davidson, L. Michelson, H. Volz, S. E. Zimmerman, E. J. Belair and A. P. Truant, *J. Med. Chem.*, 1970, **13**, 886

8 M. Boca, P. Baran, R. Boca, H. Fuess, G. Kickelbick, W. Linert, F. Renz and I. Svoboda, *Inorg. Chem*. 2000, **39**, 3205.

9 , C. Lepetit, S. Shova, F. Dahan and J.-P. Tuchagues, *Inorg. Chem*. 2005, **44**, 8916

10 A. Göblyös, L. Lázár, F. Fülöp, *Tetrahedron* 2002, **58**, 1011.

11 J. Sinkkonen, K. N. Zelenin, A. A. Potapov, I. V. Lagoda, V. V. Alekseyev, K. Pihlaja, *Tetrahedron* 2003, **59,** 1939.

12 A. M. García-Deibe, J. Sanmartín-Matalobos, C. González-Bello, E. Lence, C. Portela-García, L. Martínez and M. Fondo, *Inorg. Chem*. 2012, **51**, 1278.

13 M. Fondo, C. Portela-García, A. H. Baleeiro-Tadiotto, A. M. García-Deibe and J. Sanmartín-Matalobos, *Eur. J. Inorg. Chem*. 2015, **16**, 2744.

14 J. Sanmartín, F. Novio, A. M. García-Deibe, M. Fondo, M. R. Bermejo, J. Sanmartín, F. Novio, A. M. García-Deibe, M. Fondo and M. R. Bermejo, *New J. Chem.*, 2007, **31**, 1605.

15 H. Pizzala, M. Carles, W. E. E. Stone and A. Thevand, *J. Chem. Soc*., *Perkin Trans. 2*, 2000, 935.

16 M. Carles, F. Mansilla-Koblavi, J. A. Tenon, T. Y. N'Guessan and H. Bodot. *J. Phys. Chem*. 1993, **97**, 3716.

17 A. Jeffrey, *An Introduction to Hydrogen Bonding*, Oxford University Press, Oxford, 1997.

18 T. Steiner, *Angew. Chem. Int. Ed*. 2002, **41**, 48.

19 P. Gilli, L. Pretto, V. Bertolasi and G. Gilli, *Acc. Chem Res*. 2009, **42**, 33.

20 G. Gilli, V. Bertolasi and P. Gilli, *Cryst. Growth Des*. 2013, **13**, 3308.

21 V. I. Minkin, A. V. Tsukanov, A. D. Dubonosov and V. A. Bren, *J. Mol. Struct.* 2011, **998,** 179.

22 T. Fujiwara, J. Harada and K. Ogawa, *J. Phys. Chem. B* 2004, **108**, 4035.

23 A. T. Çolak, M. Taş, G. İrez, O. Z. Yeşilel and O. Büyükgüngör, *Z. Anorg. Allg. Chem.* 2007, **633**, 504.
24 J. Sanmartín-Matalobos, C. Portela-García, L. Martínez, C. González-Bello, E. Lence, A. M. García-Deibe and M. Fondo, *Dalton Trans*. 2012, **41,** 6998.
25 K. A. Brameld, B. Kuhn, D. C. Reuter and M. Stahl, *J. Chem. Inf. Model*. 2008, **48**, 1.
26 M. C. Burla, R. Caliandro, M. Camalli, B. Carrozzini, G. L. Cascarano, L. De Caro, C. Giacovazzo, G. Polidori and R. Spagna, *J. Appl. Crystallogr*., 2005, **38**, 381.
27 G. M. Sheldrick, SHELX2013 Programs for Crystal Structure Analysis, *Acta Cryst. A*, 2008, **64**, 112.